

PAPER • OPEN ACCESS

The uni-axial tensile response of titanium-based fiber metal laminates

To cite this article: A P Sharma and R Velmurugan 2020 *J. Phys.: Conf. Ser.* **1474** 012030

View the [article online](#) for updates and enhancements.

A promotional banner for the 240th ECS Meeting. The banner features a colorful striped border at the top. On the left, the ECS logo is displayed in a green circle. To its right, the text reads "240th ECS Meeting" in large blue font, followed by "Oct 10-14, 2021, Orlando, Florida" in a smaller blue font. Below this, it says "Register early and save up to 20% on registration costs" in bold black font, and "Early registration deadline Sep 13" in a smaller black font. At the bottom left, there is a red "REGISTER NOW" button. On the right side of the banner, there is a photograph of a diverse group of people in a professional setting, with a man in a white shirt and tie clapping and smiling in the foreground.

ECS **240th ECS Meeting**
Oct 10-14, 2021, Orlando, Florida
**Register early and save
up to 20% on registration costs**
Early registration deadline Sep 13
REGISTER NOW

The uni-axial tensile response of titanium-based fiber metal laminates

A P Sharma* and R Velmurugan

Indian Institute of Technology Madras, Chennai, India

E-mail: *ankushsharma1000@gmail.com

Abstract. Fiber metal laminates (FMLs) consist of thin layers of metal bonded together with layers of composite based on fiber reinforcement. In the present study, titanium sheets (Ti-6Al-4V) having thicknesses of 0.2 mm, 0.4 mm, and 0.6 mm and glass-fiber reinforced composite layers having uni-directional layup are considered to fabricate FMLs and response of these laminates are evaluated under tension. The consideration for four discrete sequences of stacks is made for FMLs preserving thickness of a total layer of metal same and these laminates are fabricated using a method of hand layup. The elastic modulus, yield strength and ultimate strength of FMLs are theoretically predicted by rule of mixtures (ROM). The layup's sequence does not affect initial modulus of FMLs subjected to tension. Whereas, the ultimate strength and FMLs' behavior succeeding ultimate strength are significantly affected by layup's sequence. The properties of a laminate obtained from experiment and predicted from ROM are found in good agreement with each other.

1. Introduction

Metal and fiber polymer composite with their alternating layers are used to constitute a group of materials that are hybrid and known as Fiber metal laminates (FMLs) [1]. The skin elements of Airbus A380 extensively considers currently used GLARE (glass fiber reinforced aluminium laminates) [2]. A high static [3, 4], strength with fatigue in relation to density [5–7] and resistance to corrosion [8] are the characteristics exhibited by these laminates. FMLs based on aluminium alloy are the series which is most common and broadly applied. This includes GLARE, ARALL (aramid fiber reinforced aluminium laminates), CARALL (carbon fiber reinforced aluminium laminates) and BARALL (basalt fiber reinforced aluminium laminates). However, the temperature in operation and tolerance to damage are limited for FMLs of such types. For these purposes, the necessities of a fighter plane with high speed and temperature that is high (177°C) are met by developing FMLs based on titanium known as hybrid titanium composite laminate (HTCL) [9]. The study of mechanical properties of FMLs based on titanium is then carried out by various researches, e.g. tension under quasi-static loading.

Miller et al. [9] have reported that HTCL can appear to offer a tougher, stiffer and more tolerance to damage for substitution to materials which are monolithic at higher temperatures. Adding to this, a reduction in weight and properties which are essential for applications to high-speed airliner to be established henceforth. The findings reported by Miller et al. [9] can also be found in a study performed by Li and Johnson [10]. Veazie et al. [11] have reported that improvement is shown by systems consisting of titanium with many thinner layers to titanium with fewer thicker layers. In this case, higher strength-to-weight ratios are considered



as a key concern for applications to aircraft which is high-speed and to be developed in the future. Overall, presented systems of HTCL provide a stronger substitute to equivalent metals which are monolithic. They have found that the experimental Young's modulus and strength of systems for HTCL are in good agreement with presented predictions of laminate's analysis. Papakonstantinou and Katakalos [12] have stated that the strengths and stiffnesses of FMLs based on titanium and high modulus carbon fiber are stronger and stiffer to their constituent materials with the sum of their discrete strengths and stiffnesses. Only local delamination is apparent as a secondary mode of failure succeeding fracture of fiber. After this fracture of fiber, titanium breaks at a significantly higher strain due to its ductility implying laminate's failure which does not seem catastrophic.

Bourlegat et al. [13] have investigated that laminates of titanium/carbon fiber/epoxy (CF-E) with their Young's modulus and stress under tensile loads are greater than that of GLARE and CARALL. They have reported that this hybrid material's modulus found from the experiment is agreed well to that of calculated using the rule of mixtures (ROM). Reiner et al. [14] have stated that in case of $[\text{Ti}/0/90]_s$ sample of HTCL, debonding, matrix crack's combination and pull-out of fiber are major modes of failure detected with layers of CFRP (carbon fiber reinforced polymer) having a unidirectional layup. Sharma et al. [15] have investigated that FML having layers of composite placing together exhibits higher strength under tension (GLARE-1) than FML having layers of composite isolated by layers of metal (GLARE-2 and GLARE-3). More progressive failure is exhibited by GLARE-3 after maximum stress in which layers of composite with different orientations of fiber are isolated by layers of metal. The more relevant literature associated with quasi-static tensile behavior and failure of HTCL can also be found in [16–24].

In studies performed above, behavior of FMLs is inspected by various considerations such as metal and composite with variation of their layers' number, volume fractions, etc. In the present study, FMLs are prepared by arranging layers of metal at different places across the thickness of FML maintaining total thickness of metal layers same and their behavior is investigated when subjected to quasi-static tensile loading. Digital imaging and digital image correlation (DIC) technique are used to record the real progression of damage and to measure deformation by performing correlation of images, respectively. The laminate properties are theoretically predicted using the rule of mixtures (ROM) and compared with that of obtained from experiments. The sections presented below entail specifics of work.

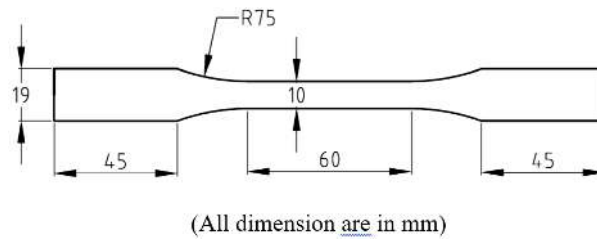
2. Experimental procedure

2.1. Specimen configurations

Titanium (Ti) alloy sheets (Ti-6Al-4V) having 0.2 mm, 0.4 mm, and 0.6 mm thicknesses are considered as the layers of metal in FML. Strength-to-weight properties are higher for Ti and at higher temperatures, Ti is much durable than aluminium [25]. The layers of composite used are uni-directional (UD) E-glass fiber reinforced epoxy (GFRP). FMLs with four dissimilar sequence of stacks are prepared through a technique of hand layup followed by compression molding maintaining the same thickness of total layers of metal. The considered sequence of stacks for FMLs and their average thickness are shown in table 1. In descriptions of FML layups provided in table 1, T6, T4 and T2 denote layers of titanium having a thickness of 0.6 mm, 0.4 mm, and 0.2 mm, respectively and 0 and 90 specify layers of UDGFRP with fibers orienting along 0° and 90° directions. Layups of FML with details of their terminology can be found in Ref. [26]. The volume fraction of fiber for composite laminate is found out to be about 50% using a burn test. The specimen of dog-bone shape is considered for testing of FML as shown in figure 1 [15].

Table 1. Details of considered FMLs.

FMLs	Layup	Ti thickness (mm)	Total thickness (mm)
2/1-0.6	[T6/0/90/90/0/T6]	0.6 + 0.6	3.05
3/2-0.4	[T4/0/90/T4/90/0/T4]	0.4 + 0.4 + 0.4	3.04
4/3-0.2(O)	[T2/0/T4/90/90/T4/0/T2]	0.2 + 0.4 + 0.4 + 0.2	3.18
4/3-0.4(O)	[T4/0/T2/90/90/T2/0/T4]	0.4 + 0.2 + 0.2 + 0.4	3.16

**Figure 1.** The geometry of the specimen for FML

2.2. Testing

The universal testing machine is used to conduct quasi-static tensile tests of FMLs at a cross-head speed of 1 mm/min at room temperature. During testing, events of failure are recorded by visualizing FMLs' edges using two mirrors as can be seen in figure 2a. A pattern of random nature (speckle of black on a background of white) is applied to the specimen using paint in spray form as presented in figure 2b. Uniform illumination is obtained on the specimen's surface by using a pair of lamps placed each on camera's either side (Edmund optics). The load is matched with images by recording corresponding output from load cell by image grasping software every time an image is bagged. An image correlation software named Vic-2D supplied by Correlated Solutions, Inc. is used to get strain field when subjected to quasi-static loading by using a CCD camera delivered by Point Grey. Displacements along the axial direction of two points detached by a distance which is recognized and surrounded by gage area are taken out for each load to acquire corresponding engineering strain. This engineering strain has been used by subsequent figures of stress-strain relationships.

3. Results

Typical stress-strain behavior and failure patterns of FMLs, when subjected to tensile loading, will be presented in this section together with theoretical predictions of FMLs' properties.

3.1. The behavior of FMLs in terms of stress-strain

3.1.1. FML 2/1-0.6. An experimental stress-strain behavior which is typical of FML 2/1-0.6 having lay-up [T6/0/90]_s is shown in figure 3. Initially, the stress-strain curve of FML shows a linear behavior followed by a hardening behavior which seems non-linear till attaining of maximum stress. The layer of titanium yields when FML's stress reaches 415 MPa. Therefore, the deviation from a region which is linear is equivalent to yielding for a layer of titanium as can be seen in the experiment. The slope continuously decreases up to about 457 MPa followed by a response which seems linear up to about 524 MPa and further constantly decreases till reaching the level of stress which is maximum of 530 MPa. The photographs of the specimen equivalent to levels of stress shown by open circles indicating with points A–D are presented in figure 4 in the same sequence. The specimen's view at its edge in figure 4a corresponding to the stress

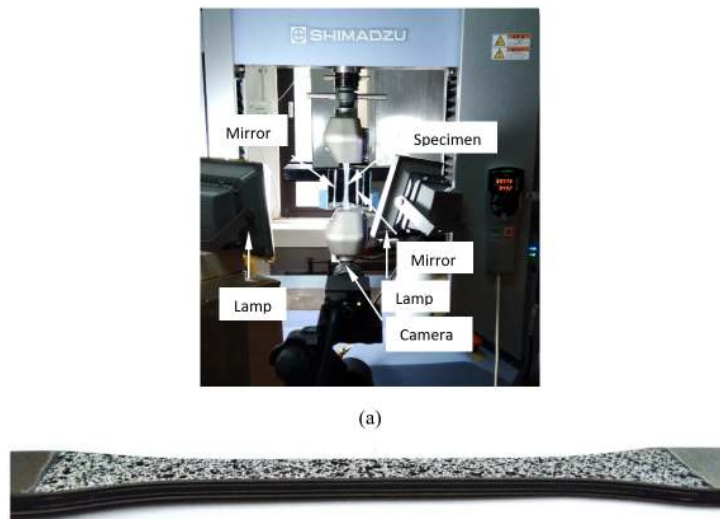


Figure 2. (a) Experimental setup, (b) FML 4/3-0.4(O) specimen having a pattern of DIC

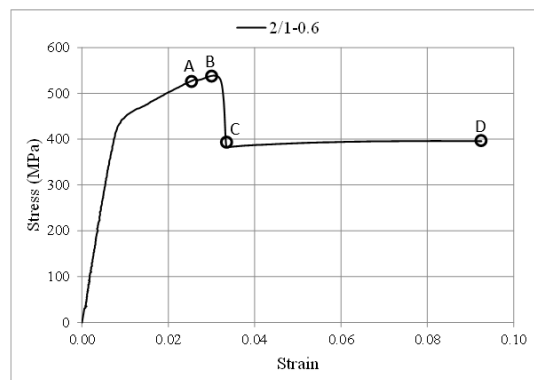


Figure 3. The behavior of FML 2/1-0.6 under tensile loading

level of 530 MPa does not exhibit any noticeable damage of significant extent. The specimen's photograph corresponding to the stress level of 530 MPa is shown in figure 4b. In this case, splitting and failure of fiber for composite layers with fibers orienting along 0° direction (0C) are observed causing delamination between T6 and 0C designating by a white arrow. Therefore, the sudden dropping of stress is resulted by the failure of 0C. With further deformation of the specimen, more amount of splitting and fracture of fiber for 0C are occurred corresponding to a level of stress of 385 MPa as shown in figure 4c. Following this, sheets of titanium share majority of load and stress which increases gradually is evident (figure 3). This sharing of the load is exhibited by sheets of titanium until both layers of titanium fail. The strain which is being localized for one sheet of titanium marked by an elliptical symbol is shown in figure 4d just before failure.

3.1.2. FML 3/2-0.4. Typical stress-strain behavior of FML 3/2-0.4 with layup [T4/0/90/T4/90/0/T4] is shown in figure 5. The specimen's photograph analogous to points A–H indicating by open circles in figure 5 are presented in figure 6 in the same order. Akin to FML 2/1-0.6, the stress-strain curve shows a response which is linear initially up to about 401 MPa till stress for FML's titanium layer reaches yield stress of titanium following behavior

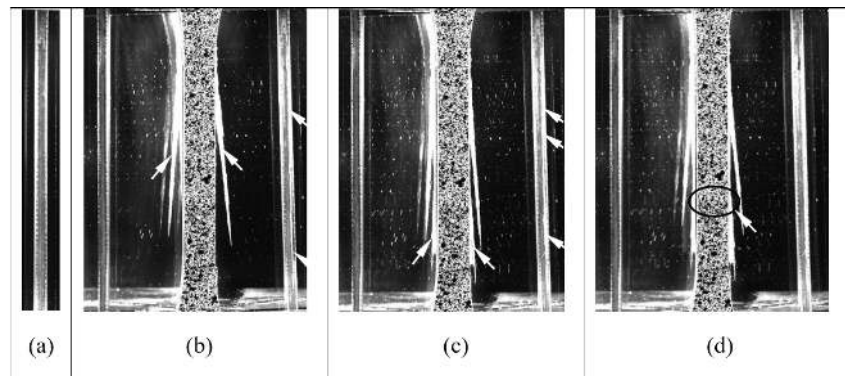


Figure 4. Photographs showing damage evolution for FML 2/1-0.6

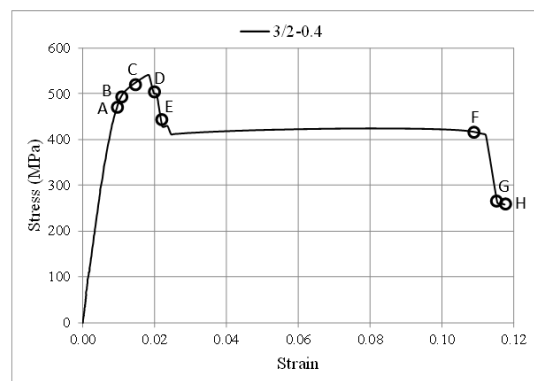


Figure 5. The response of FML 3/2-0.4 under tensile loading

which seems non-linear. Dropping of stress has happened after a level of stress that attains maximum value. The specimen's edge view shown in figure 6a before reaching the stress level that is maximum exhibits no visible damage. The photograph of the specimen equivalent to a level of stress of 488 MPa before reaching maximum stress is shown in figure 6b. In this case, initiation of delamination is taken place between composite layers with fibers orienting along 90° direction (90C) and middle T4 indicating by the white arrow (figure 6b). This is followed by more amount of delamination between 90C and middle T4 as can be seen in figure 6c. With continuous deformation of the specimen, splitting and failure of fiber for one layer of 0C are observed causing delamination between 0C and T4 (figure 6d). Following this, the level of stress drops to 429 MPa with increasing strain at which splitting and failure of fiber for another layer of 0C are observed causing delamination between 0C and T4 (figure 6e). Afterward, the stress further drops to a level of 412 MPa followed by sharing of load by titanium layers. The stress level then gradually rises to 415 MPa with increasing strain at which cracking is initiated for middle T4 corresponding to point F as shown in figure 5 (figure 6f). This is continued with stress level which gradually decreases to 410 MPa following dropping of stress level to 263 MPa at which fracture of middle T4 has happened (figure 6g). The stress level again drops to 259 MPa where localization of strain is observed for one layer of T4 as shown by an elliptical symbol and this layer is about to fail (figure 6h). Following stress level which is maximum for FML, failure of progressive nature is observed for FML 3/2-0.4 to FML 2/1-0.6. Layers of the composite are not failed at a single time for FML 3/2-0.4, as substitute, stepwise failure is observed for them causing dipping of stress levels in two steps.

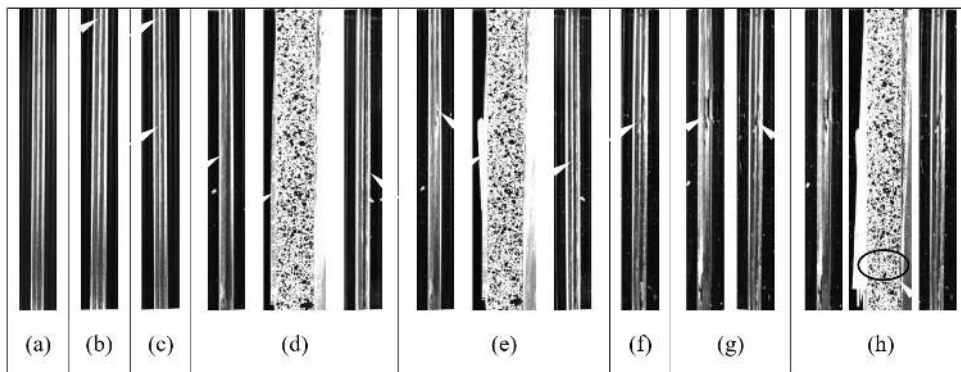


Figure 6. Photographs showing damage development for FML 3/2-0.4

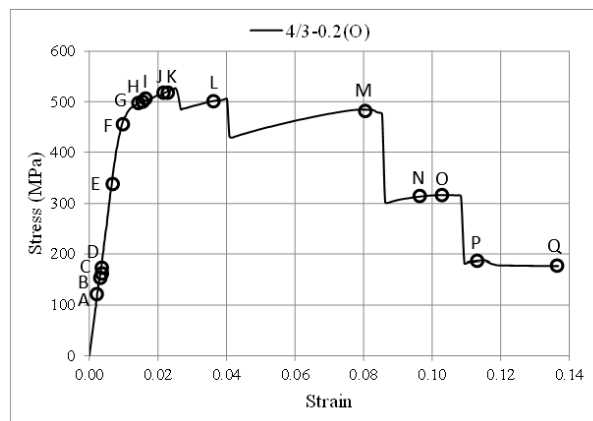


Figure 7. The behavior of FML 4/3-0.2(O) under tension

3.1.3. FML 4/3-0.2(O). The typical behavior of stress-strain for FML 4/3-0.2(O) having layup $[T2/0/T4/90]_s$ is shown in figure 7 where circles which are open are marked by points A–Q that are equivalent to the specimen's photographs presented in figure 8 exhibiting a progression of damage. The initial behavior obtained for this FML till attainment of stress which is maximum seems analogous to FML 2/1-0.6 and FML 3/2-0.4. The left side view (L) and right side view (R) of the specimen with no evidence of damage are shown in figure 8a equivalent to a level of stress of 117 MPa. Consequently, initiation of matrix cracking takes place for 90C reinforcing between two layers of titanium (T4) analogous to a level of stress of 147 MPa labelling by a white arrow in figure 8b. With rising deformation of the specimen, matrix cracking of more amount is appeared corresponding to a stress level of 153 MPa as can be noted in figure 8c. Afterward, these matrix cracks can be seen for 90C conforming to a level of stress of 159 MPa causing initiation of delamination between 90C and T4 in figure 8d. This causes delamination to more extent between 90C and T4 consistent to a level of stress of 335 MPa as can be illustrated in figure 8e. This is followed by the initiation of splitting and failure of fiber for one layer of 0C at a level of stress of 453 MPa causing initiation of delamination between 0C and T2 as noted in figure 8f.

After this, initiation of splitting and failure of fiber for another layer of 0C have occurred at a stress level of 498 MPa producing initiation of delamination between 0C and T2 as can be seen in figure 8g. The successive loading of the specimen exhibits more amount of splitting and failure of fiber for both layers of 0C corresponding to a level of stress of 500 MPa as shown in

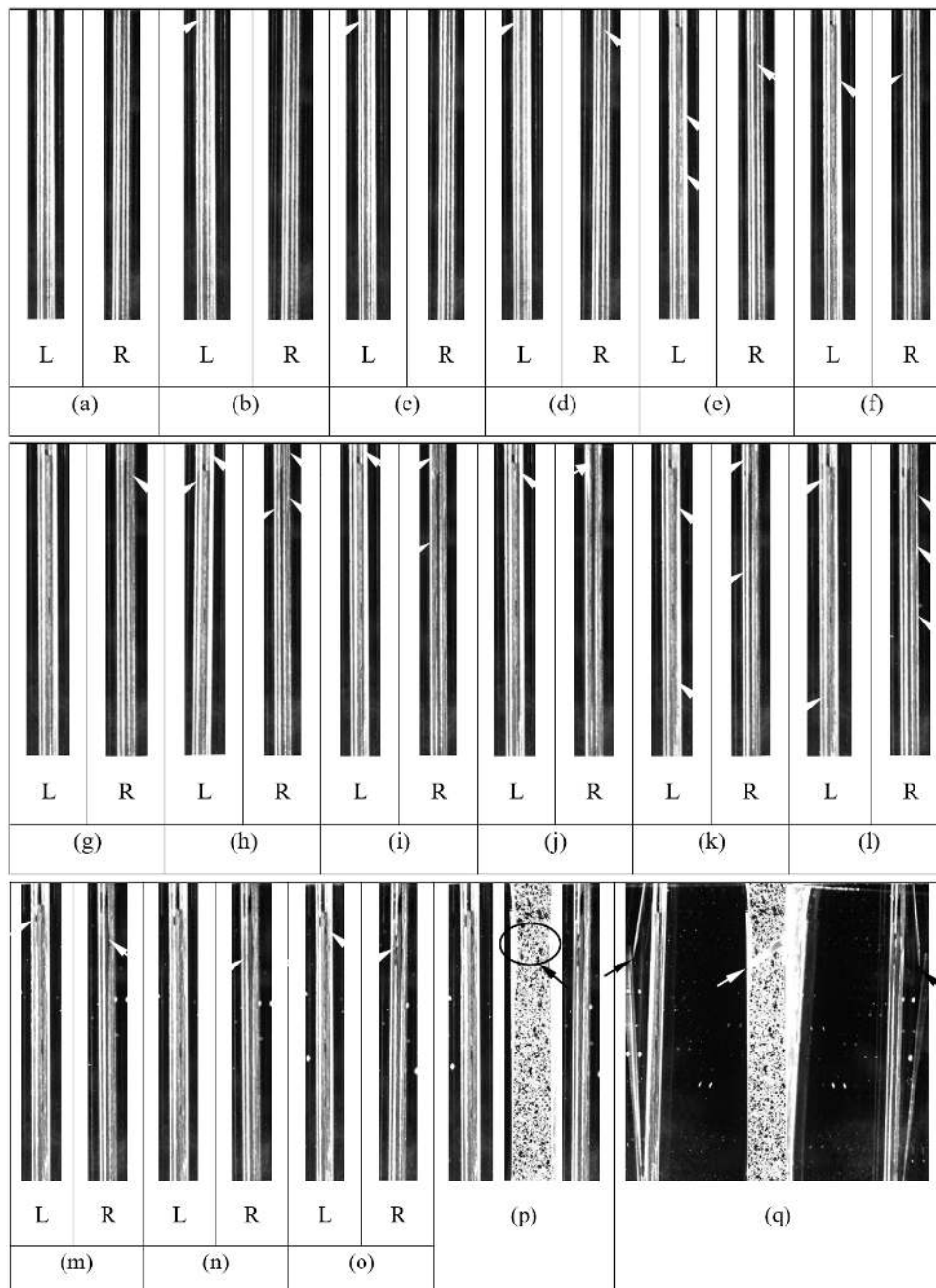


Figure 8. Photographs showing a progression of damage for FML 4/3-0.2(O)

figure 8*h*. This triggers more amount of delamination between both layers of 0C, T4, and T2 (figure 8*h*). The loading is continued with splitting and failure of fiber to a large extent for one layer of 0C at a level of stress of 507 MPa bringing a large amount of delamination between 0C and T4 to figure 8*h* (figure 8*i*). Successively, fracture of fiber is occurred for one layer of 0C parallel to a stress level of 521 MPa producing delamination to large extent between 0C, T2, and T4 to figure 8*i* (figure 8*j*). The specimen then exhibits a large amount of fiber fracture for one layer of 0C to figure 8*j* causing small dropping of a curve at a level close to a maximum stress of 524 MPa (figure 7) as can be seen in figure 8*k*. Along with this, an extensive amount of

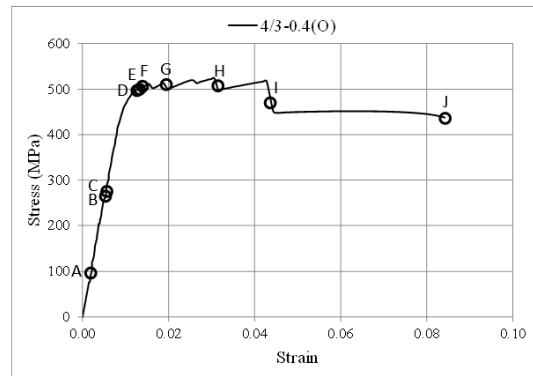


Figure 9. The behavior of FML 4/3-0.4(O) under tension

delamination is caused between 0C, T4, and T2 to figure 8j (figure 8k). The stress level then drops to 486 MPa and rises to 503 MPa with increasing strain at which a large amount of fiber fracture for another layer of 0C is revealed in figure 8l. This brings about a significant amount of delamination between 0C, T2, and T4 (figure 8l).

The stress level then reaches to 505 MPa and dips to 429 MPa followed by a gradual increase in stress to a level of 484 MPa with more amount of rising strain shared by titanium layers at which fracture of one layer of T4 has happened (figure 8m). With continuous sharing of load by titanium layers, stress level reaches to 476 MPa and further drops to a level of 301 MPa and gradually increases to 315 MPa with increasing strain where localization for another layer of T4 becomes apparent (figure 8n). The loading event is continued with stress reaching to a level of 316 MPa at which fracture for another layer of T4 is occurred (figure 8o). Consecutively, a stress level reaches to 314 MPa followed by a continuous fall to 184 MPa and slowly rises to 187 MPa at which localization for one layer of T2 is evident as marked by an elliptical symbol (figure 8p). The specimen finally elongates steadily to a strain of 13.7% and attains a stress level of 177 MPa where fracture for one layer of T2 is noted (figure 8q).

3.1.4. FML 4/3-0.4(O). Layers of the same type are considered in this FML 4/3-0.4(O) to FML 4/3-0.2(O) with the exception that titanium with their outer layers used is thicker ones. The behavior of FML 4/3-0.4(O) with layup $[T4/0/T2/90]_s$ which is typical is shown in figure 9 where marking of open circles are indicated by points A–J at different levels of stress. The conforming representations for progression of damage are depicted in figure 10 in the same order. For this FML, behavior attained initially until the level of maximum stress is analogous to FMLs 2/1-0.6, 3/2-0.4 and 4/3-0.2(O). The specimen without exhibiting any visible damage is shown in figure 10a equivalent to a level of stress of 94 MPa. The successive loading of the specimen leads to the origination of matrix cracking at a level of stress conforming to 265 MPa as can be seen in figure 10b. This causes initiation of delamination between 90C reinforcing between two titanium layers (T2) and adjacent T2 (figure 10b). The specimen then reveals more amount of matrix cracking for 90C akin to a level of stress of 275 MPa in figure 10c. This produces more amount of delamination between 90C and adjacent T2 designating by a white arrow (figure 10c).

Consequently, initiation of splitting and failure of fiber are revealed for one layer of 0C parallel to a level of stress of 500 MPa as can be noticed in figure 10d. This causes initiation of delamination between 0C and adjacent T2 (figure 10d). The continuous deformation of the specimen then exhibits more amount of splitting and failure of fiber for one layer of 0C at a level of stress of 502 MPa as shown in figure 10e. This is followed by correspondingly a more amount of delamination between 0C and T2 (figure 10e). The specimen then stretches and exhibits

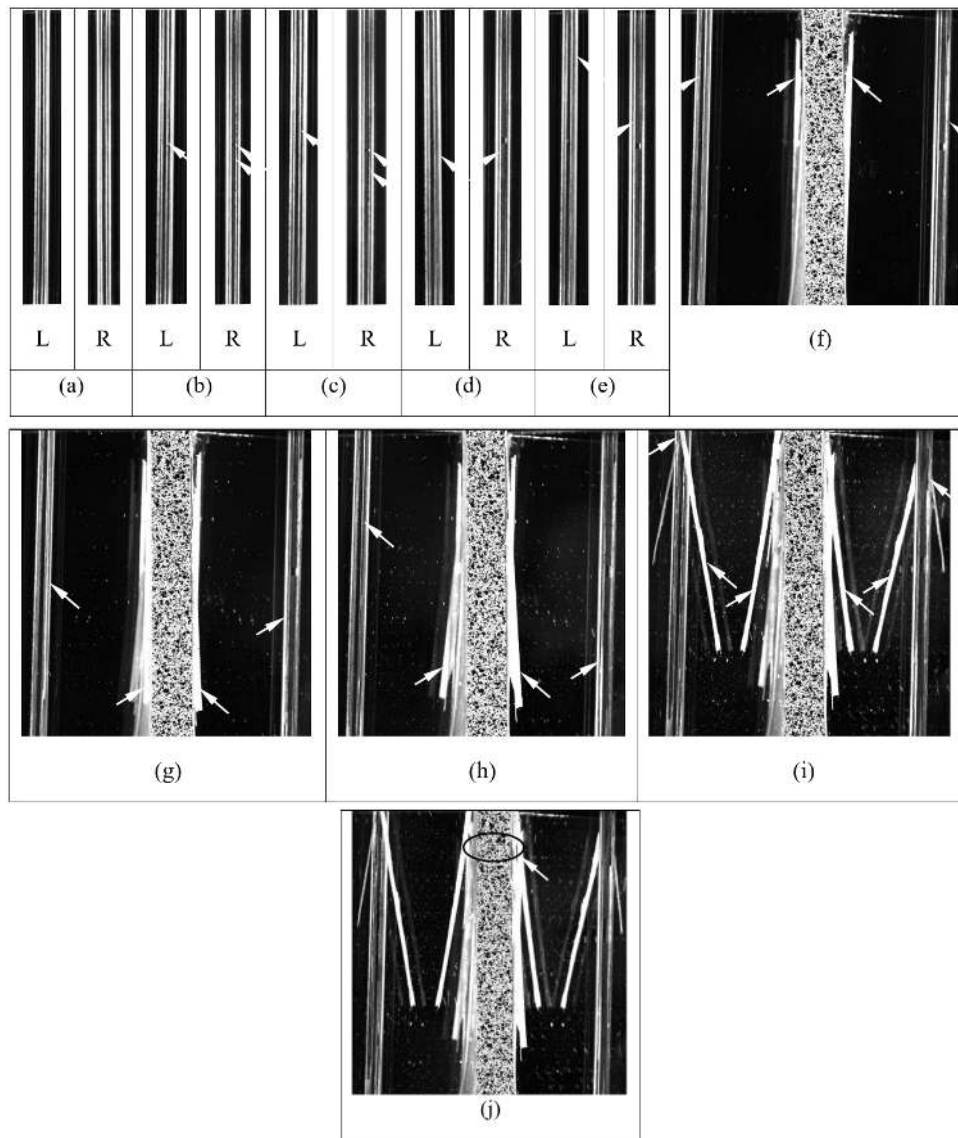


Figure 10. Images of damage development for FML 4/3-0.4(O)

splitting and failure of fiber for another layer of 0C at a stress level consistent to 512 MPa causing small dropping of stress with the increasing strain (figure 9) and also delamination between 0C, adjacent T2 and T4 (figure 10f). The successive loading exhibits splitting and fracture of fiber for one layer of 0C at a level of stress equivalent to 501 MPa causing another small dipping of stress (figure 10g). This causes delamination to large extent between 0C, adjacent T4 and T2 to figure 10e (figure 10g). The further event of failure includes more amount of splitting and fracture of fiber for one layer of 0C at a stress level of 500 MPa exhibiting successive dropping of stress with the rising strain (figure 10h). This causes an extensive amount of delamination between 0C and adjacently located T4 and T2 to figure 10g (figure 10h). The continuous elongation of the specimen results into a stress level that increases to 518 MPa with growing strain and then drops to 451 MPa at which significant amount of fiber fracture is unveiled for another layer of 0C (figure 10i). This causes a large amount of delamination between 0C, adjacent T4 and T2 (figure 10i). The level of stress then drops to 448 MPa followed by a gradually increasing load

with sharing of the bulk of the load by titanium layers. This event then reaches to a stress level of 438 MPa at which localization of strain is noted for one layer of T4 as marked by an elliptical symbol and is about to fail as can be noticed in figure 10j.

3.2. Theoretical prediction of tensile properties of FMLs

The elastic modulus of FML is predicted by the rule of mixtures (ROM) when subjected to in-plane quasi-static tensile loading condition using equation (1) as follows [1, 24]:

$$(E)_{\text{FML}} = MVF(E)_{\text{T}} + (1 - MVF)(E)_{\text{FRP}} \quad (1)$$

where $(E)_{\text{FML}}$, $(E)_{\text{T}}$, and $(E)_{\text{FRP}}$ are corresponding moduli of FML, titanium sheets, and GFRP composite $[0/90]_s$. The ratio of the sum of thicknesses of separate layers of titanium and total laminate's thickness is known as metal volume fraction, see equation (2) [1].

$$MVF = \frac{\sum_1^P t_{\text{T}}}{t_{\text{FML}}} \quad (2)$$

Where MVF is metal volume fraction for a layer of titanium, t_{T} is metal layer's thickness, P is the number of metal layers, and t_{FML} is the thickness of FML. Similarly, the yield strength of FML is calculated by ROM using equation (3) as follows [24]

$$(\sigma_y)_{\text{FML}} = MVF(\sigma_y)_{\text{T}} + (1 - MVF)(\sigma_y)_{\text{FRP}}, \quad (3)$$

where $(\sigma_y)_{\text{FML}}$, $(\sigma_y)_{\text{T}}$, and $(\sigma_y)_{\text{FRP}}$ are yield strengths of FML, titanium sheets, and GFRP composite $[0/90]_s$. For a linear elastic kind of behavior for FML where the behavior of linear kind is considered for both layers of titanium and FRP, strain experienced by FML and its constituents is equal. Therefore,

$$\varepsilon_{\text{FML}} = \varepsilon_{\text{T}} = \varepsilon_{\text{FRP}}. \quad (4)$$

This strain can be written in terms of stress and elastic modulus for composite layers and titanium sheets using Hooke's law since all layers of FML exhibit one-dimensional nature of stress as follows

$$(\sigma_y)_{\text{FRP}}(E_{\text{FRP}})^{-1} = (\sigma_y)_{\text{T}}(E_{\text{T}})^{-1}. \quad (5)$$

This can be simplified as follows

$$(\sigma_y)_{\text{FRP}} = (\sigma_y)_{\text{T}}(E_{\text{FRP}})(E_{\text{T}})^{-1}. \quad (6)$$

Substituting this value of $(\sigma_y)_{\text{FRP}}$ in equation (3),

$$(\sigma_y)_{\text{FML}} = [MVF + (1 - MVF)(E_{\text{FRP}})(E_{\text{T}})^{-1}](\sigma_y)_{\text{T}}. \quad (7)$$

The identification of stress at the point of the knee of a stress-strain curve which seems approximately bilinear (figures 3, 5, 7, and 9) is used to find out the experimental strength at yield point of FMLs. The ultimate strength of FML is calculated by ROM using equation (8) as follows [1, 24]

$$(\sigma_u)_{\text{FML}} = MVF[(\sigma_u)_{\text{T}}]_{\varepsilon_{\text{FRP}}^*} + (1 - MVF)(\sigma_u)_{\text{FRP}}, \quad (8)$$

where $(\sigma_u)_{\text{FML}}$, $[(\sigma_u)_{\text{T}}]_{\varepsilon_{\text{FRP}}^*}$, and $(\sigma_u)_{\text{FRP}}$ are ultimate strengths of FML, titanium sheets at failure strain of GFRP composite $([0/90]_s)$ and GFRP composite $[0/90]_s$, respectively. Elastic modulus and yield strength of FMLs are calculated by using equations (1) and (7) considering corresponding moduli and yield strengths of titanium sheets and $[0/90]_s$ composite laminate as

Table 2. Tensile properties of FMLs' constituents.

Material	Elastic modulus (GPa)	Yield strength (MPa)	Ultimate strength (MPa)	Specific stiffness (GPa/(kg/m ³))
[0/90] _s laminate	015	–	0653 ^a	0.0090
T2	112	0917	0967 ^b	0.0253
T4	119	1008	1040 ^b	0.0269
T6	117	0984	1005 ^b	0.0264

^aUltimate strength of [0] composite laminate.

^bUltimate strength of titanium sheets at failure strain of [0] composite laminate (i.e., at 0.0202).

Table 3. Comparison of tensile properties of FMLs.

Material	Elastic modulus (GPa)		Yield strength (MPa)		Ultimate strength (MPa)		Specific stiffness (GPa/(kg/m ³))
	Experi- ment	Theory	Experi- ment	Theory	Experi- ment	Theory	
2/1-0.6	54.3	55.1	459 ± 08	462	545 ± 14	592	0.0196
3/2-0.4	54.3	56.3	454 ± 34	476	521 ± 18	609	0.0196
4/3-0.2(O)	51.6	52.7	474 ± 29	436	535 ± 17	577	0.0190
4/3-0.4(O)	52.2	53.7	470 ± 09	448	520 ± 26	588	0.0190

tabulated in table 2. In case of ultimate strength of FMLs, since composite layer with fibers orienting along 90° direction 90C fail early during loading of FMLs, their contribution to the overall strength of FMLs is very small and therefore is excluded. Thus, the ultimate strength of FMLs is estimated by using equation (8) considering corresponding strengths of titanium sheets at failure strain of [0] composite laminate (i.e., at 0.0202) and [0] composite laminate as tabulated in table 2. It is observed that the difference between average values of elastic modulus, yield strength and ultimate strength of FMLs obtained from experiment and ROM's calculations is about 4%, 8%, and 17%, respectively as can be seen in table 3. In this case, the value of properties obtained from experiments are on the lower side in most of the cases (table 3). In case of difference between experimental and theoretical ultimate strength of FMLs, assumption of simultaneous failure for layers of titanium and FRP is made in ROM's calculations, however, this does not happen in case of experiments. Also, since the influence of interface or void's occurrence is not considered for layers of FRP in calculations of ROM, the difference is occurred between experimental and predicted values of tensile properties of FMLs. Apart from this, consideration to model debonding between metal and FRP layers is not accounted for.

4. Discussion

In this section, the tensile response of four FMLs is compared based on a different sequence of stacks. Metal layers' placement within laminate does affect the tensile behavior of FMLs, especially in the area ahead of yielding of metallic layers as can be noticed from results obtained in sections 3.1 and 3.2. From table 3, it can be noted that strength is slightly higher for FML 2/1-0.6 to FMLs 3/2-0.4, 4/3-0.2(O) and 4/3-0.4(O). This suggests that the dispersion of composite layers by metal layers yields somewhat lower strengths for FML 3/2-0.4 and both FMLs 4/3. The observation of strength's reduction mainly comes from table 3 reporting averages values.

Further observation consists of bilinear response for FMLs 4/3-0.2(O) and 4/3-0.4(O) including a slope alteration after the beginning of titanium layers' yielding as can be noticed in figures 7 and 9. On the other hand, small constant reduction of slope happens with the strain which is growing after titanium layers' yielding till attaining maximum stress as can be observed in figures 3 and 5. The interpretation of this behavior is as follows. Formation of matrix cracks within 90° layers after attaining transverse strength by this layer can be stably extended into an in-line layer of 0° even bridging of fibers happen by this 0° layer. Because of this, a degradation would be experienced by the stiffness of 0° layers and subsequently that of FML. This results in the behavior of change of slope which seems to have a constant reduction for FMLs 2/1-0.6 and 3/2-0.4 particularly before attaining maximum stress (figures 3 and 5).

In the case of FML 3/2-0.4, since the insulation of two layers of 90° is done by a layer of titanium, statistically different form of cracking is predicted to be exhibited by these two layers of 90° . This causes separate degradation for the stiffness of layers of 0° which are in-line due to the crossing of matrix cracks into them. This will result in different values of strain for the failure of layers of 0° as noted in experiments. In comparison to this, in the case of FMLs 4/3-0.2(O) and 4/3-0.4(O), the only location of the layer of titanium is changed, i.e., thinner and thicker titanium layers are located on layers which are outer and inner for FML 4/3-0.2(O) and vice versa for FML 4/3-0.4(O). In these cases of FMLs 4/3, layers of 0° and 90° are not placed adjacent and isolated by layers of titanium. Due to this, the crossing of matrix cracks within layers of 90° cannot happen into layers of 0° , thus stiffness for layers of 0° has not resulted in a degradation. Therefore, in this case, progressive reduction in slope is not observed near peak stress in the relationship of stress-strain (figures 7 and 9) as that observed for FMLs 2/1-0.6 and 3/2-0.4 (figures 3 and 5).

Tabulating assessment of specific stiffness which is the ratio of elastic modulus to volume density amongst sheets of monolithic titanium, $[0/90]_s$ composite laminate and FMLs is shown in tables 2 and 3. It is observed that monolithic titanium sheets such as T2, T4 and T6 are having similar and higher specific stiffness to that of FMLs. On the other hand, FML of all cases is having similar and higher specific stiffness to that of a cross-ply laminate of composite $[0/90]_s$. This means that FMLs with their specific stiffness shows an enhancement over $[0/90]_s$ composite laminate.

5. Conclusions

The stress-strain behavior of four discrete layups of FMLs is presented along with their real-time damage evolution. The effect of layers of metal dispersing through the thickness on the behavior of FMLs is brought out under tension preserving total thickness for a layer of metal same. FMLs properties are theoretically predicted using the rule of mixtures and compared with experimental results. The present study shows the following.

The strength of FML having placement of layers of composite together (FML 2/1-0.6) is higher than that of FMLs in which layers of metal are used to discrete layers of composite. After attaining maximum stress, FMLs display a more progressive type of failure in which layers of the composite are isolated by layers of metal. FMLs 4/3-0.2(O) and 4/3-0.4(O) exhibit the aforementioned kind of failure very noticeably. The tolerance to damage seems to increase for FMLs in which layers of composite having orientations of fiber that are not similar are separated by a layer of a metal exhibiting minor strength's reduction. The tensile properties of laminates are theoretically predicted by the rule of mixtures and results found from these calculations are in good comparison with experimental results. The specific stiffness of hybrid laminate shows an enhancement over $[0/90]_s$ composite laminate. Monolithic metals can be replaced by such hybrid laminates which are having the lower density to that of metals. Therefore, areas, where savings of weight are considered very important, can particularly use these hybrid laminates.

References

- [1] Vlot A and Gunnink J W 2001 *Fiber metal laminates: An introduction* (The Netherlands: Kluwer Academic Publishers)
- [2] Vogelesang L B and Vlot A 2000 Development of fiber metal laminates for advanced aerospace structures *J. Mater. Process. Technol.* **103** (1) 1–5
- [3] Reyes G V and Cantwell W J 2000 The mechanical properties of fibre-metal laminates based on glass fibre reinforced polypropylene *Compos. Sci. Technol.* **60** (7) 1085–94
- [4] Kawai M, Morishita M, Tomura S, and Takumida K 1998 Inelastic behavior and strength of fiber-metal hybrid composite: Glare *Int. J. Mech. Sci.* **40** (2-3) 183–98
- [5] Dadej K, Bienias J, and Surowska B 2018 Isostrain elastoplastic model for prediction of static strength and fatigue life of fiber metal laminates *Int. J. Fatigue* **110** 31–41
- [6] Dadej K, Bienias J, and Surowska B 2017 Residual fatigue life of carbon fibre aluminium laminates *Int. J. Fatigue* **100** (1) 94–104
- [7] Alderliesten R C and Homan J J 2006 Fatigue and damage tolerance issues of Glare in aircraft structures *Int. J. Fatigue* **28** (10) 1116–23
- [8] Bienias J, Jakubczak P, and Surowska B 2017 Properties and characterization of fiber metal laminates In *Hybrid Polymer Composite Materials: Properties and Characterization* (Woodhead Publishing Elsevier) pp. 253–77
- [9] Miller J L, Progar D J, Johnson W S, and Clair T S L St 1995 Preliminary evaluation of hybrid titanium composite laminates *J. Adhesion* **54** (1-4) 223–40
- [10] Li E and Johnson W S 1998 An investigation into the fatigue of a hybrid titanium composite laminate *J. Comp. Technol. Res.* **20** (1) 3–12
- [11] Veazie D, Badir A, and Grover Jr R 1998 Titanium ply effects on the behavior of a hybrid thermoplastic composite laminate *J. Thermoplast. Compos. Mater.* **11** (5) 443–54
- [12] Papakonstantinou C and Katakalos K 2009 Mechanical behavior of high temperature hybrid carbonfiber/titanium laminates *J. Engng Mater. Technol.* **131** (2) 021008
- [13] Le Bourlegat L, Damato C, Da Silva D, et al. 2010 Processing and mechanical characterization of titanium-graphite hybrid laminates *J. Reinf. Plast. Compos.* **29** (22) 3392–400
- [14] Reiner J, Veidt M, and Dargusch M 2018 Failure modes in hybrid titanium composite laminates *J. Engng Mater. Technol.* **140** 011005
- [15] Sharma A P, Khan S H, and Parameswaran V 2017 Experimental and numerical investigation on the uni-axial tensile response and failure of fiber metal laminates *Compos. Part B Engng* **125** 259–74
- [16] Cortes P and Cantwell W J 2004 The tensile and fatigue properties of carbon fiber-reinforced PEEK-titanium fiber-metal laminates *J. Reinf. Plast. Compos.* **23** (15) 1615–23
- [17] Cortés P and Cantwell W J 2006 Structure-properties relations in titanium-based thermoplastic fiber-metal laminates *Polym. Compos.* **27** (3) 264–70
- [18] Cortés P and Cantwell W J 2006 The prediction of tensile failure in titanium-based thermoplastic fibre-metal laminates *Compos. Sci. Technol.* **66** (13) 2306–16
- [19] Jen M-H R, Chang C-K, and Sung Y-C 2016 Fabrication and mechanical properties of Ti/APC-2 hybrid nanocomposite laminates at elevated temperatures *J. Compos. Mater.* **50** (15) 2035–45
- [20] Du D, Hu Y, Li H, et al. 2016 Open-hole tensile progressive damage and failure prediction of carbon fibre-reinforced PEEK-titanium laminates *Compos. Part B Engng* **91** 65–74
- [21] Wang X, Ahn J, Lee J, and Blackman B R K 2016 Investigation on failure modes and mechanical properties of cfrp-ti6al4v hybrid joints with different interface patterns using digital image correlation *Mater. Des.* **101** 188–96
- [22] Ali A, Pan L, Duan L, et al. 2016 Characterization of seawater hygrothermal conditioning effects on the properties of titanium-based fiber-metal laminates for marine applications *Compos. Struct.* **158** 199–207
- [23] Zhang J, Wang Y, Fang G, et al. 2017 Application of energy dissipation approach for notched behavior in fiber metal laminates *Compos. Struct.* **180** 809–20
- [24] Mathivanan P, Balakrishnan M, and Krishnan H 2010 Metal thickness, fiber volume fraction effect on the tensile properties, debonding of hybrid laminates *J. Reinf. Plast. Compos.* **29** (14) 2128–40
- [25] Niu W, Birmingham M, Baburamani P, et al. 2013 The effect of cutting speed and heat treatment on the fatigue life of Grade 5 and Grade 23 Ti-6Al-4V alloys *Mater. Des.* **46** 640–4
- [26] Sharma A P, Khan S H, Kitey R, and Parameswaran V 2018 Effect of through thickness metal layer distribution on the low velocity impact response of fiber metal laminates *Polym. Test.* **65** 301–12